

The Galaxy in circular polarization: all-sky radio prediction, detection strategy, and the charge of the leptonic cosmic rays

Torsten A. Enßlin,^{*} Sebastian Hutschenreuter,^{*} Valentina Vacca,[†] and Niels Oppermann[‡]

The diffuse Galactic synchrotron emission should exhibit a low level of diffuse circular polarization (CP) due to the circular motions of the emitting relativistic electrons. This probes the Galactic magnetic field in a similar way as the product of total Galactic synchrotron intensity times Faraday depth. We use this to construct an all sky prediction of the so far unexplored Galactic CP from existing measurements. This map can be used to search for this CP signal in low frequency radio data even prior to imaging. If detected as predicted, it would confirm the expectation that relativistic electrons, and not positrons, are responsible for the Galactic radio emission. Furthermore, the strength of real to predicted circular polarization would provide statistical information on magnetic structures along the line-of-sights.

I. INTRODUCTION

A. Circular polarisation emission

The radio synchrotron emission of the Milky Way should be circularly polarized due to the circular motions of relativistic electrons in the Galactic magnetic field (GMF). Because of the relativistic beaming effect of the electron's motion on the emitted radiation we see mostly the electrons that spiral around fields oriented perpendicular to the line-of-sight (LOS) and therefore predominantly linearly polarized emission. The magnetic fields that point towards us could be a source of circular polarization (CP), reflecting the circular motions of the relativistic electrons visible in this geometry. However, the aforementioned beaming effect diminishes any radiation parallel to the magnetic field. The largest CP emission should therefore result from magnetic fields with an inclination in between parallel and perpendicular to the LOS. The field component parallel to the LOS, B_{\parallel} , ensures that a circular component of the electron gyration is visible to the observer, and determines thereby the sign of Stokes-V. The field component perpendicular to the LOS, B_{\perp} , enables the gyrating electrons to send some beamed flux into the direction of the observer and therefore largely determines the strength of the CP.

So far only linear polarization has been detected and imaged in the diffuse radio-synchrotron emission of the Milky Way [1–3].¹ CP should be much weaker and therefore harder to be detected and charted. Nevertheless, Galactic CP emission should exist and there-

fore should in principle be observable. Since the CP signal is weak, and has to be discriminated from instrumental polarization leakage effects, it would be very helpful to have a prediction not only on the magnitude of this emission, but also on its detailed morphology on the sky. This paper provides such a prediction.

B. Predicting circular polarisation

To predict the CP emission accurately knowledge of the GMF strength and orientation is necessary throughout the Galactic volume, as well on the number density and the energy spectrum of the relativistic electron population. Currently we are lacking this information, despite substantial efforts to model the GMF [17–26], the Galactic thermal electrons [27, 28], and relativistic electrons [29–35] from various observables. The observables informing us about the perpendicular GMF component (times the relativistic electron density) are the linear polarization and total emission of the synchrotron emission. The parallel GMF component imprints onto the Galactic Faraday rotation measures of extra-galactic sources, however modulated by the thermal electron density. Instead of using these observables to construct a 3D GMF model from which CP can be predicted [36], here we exploit that a certain combination of these observables should be linearly correlated with the CP signal. Exploiting this correlation without the detour of building a simplified 3D GMF model should permit to predict more small-scale structures of the Galactic CP signal than by usage of a coarse 3D GMF model. The CP sky prediction by [36] is based on such a 3D model and exhibits small scale structures. The latter are, however, due to a random magnetic field added to the 3D model, and therefore will not represent the real small-scale structures of the CP sky.

The small scale-structures of our predicted CP signal will be more realistic. However, they only represent a statistical guess for the real CP signal. The pieces of information that are put together, the Faraday signal as a tracer of B_{\parallel} and the total synchrotron intensity as a tracer of B_{\perp} , might report about different locations along the LOS, whereas the combination of both components at the locations of CP emission

^{*} Max Planck Institute for Astrophysics, Karl-Schwarzschildstr.1, 85741 Garching, Germany; Ludwig-Maximilians-Universität München, Geschwister-Scholl-Platz 1, 80539 Munich, Germany

[†] Osservatorio Astronomico Cagliari, Via della Scienza 5 - 09047 Selargius, Italy

[‡] Canadian Institute for Theoretical Astrophysics; 60 St. George Street; Toronto, ON M5S 3H8; Canada Dunlap Institute for Astronomy and Astrophysics; 50 St. George Street; Toronto, ON M5S 3H4; Canada

¹ CP from compact Galactic objects like Sagittarius A*, GRS 1915, SS 433 has been detected [4–7], which seems to result from a different process as discussed here, namely Faraday conversion operating in the much stronger magnetic fields of these objects [8–16].

would be needed. The former signal results predominately from locations of high thermal and the latter of high relativistic electron density, and these do not need to coincide spatially.

Fortunately, the GMF exhibits some spatial correlation as the observables are correlated as a function of sky direction and this correlation should also hold in the LOS direction. Therefore, information on field components resulting from slightly different locations might still provide a good guess at a position. Some of the structures imprinted onto the observables are caused by structures in the underlying thermal or – to a lesser degree – relativistic electron population and might, however, be misleading and lead to spurious structures in a CP sky predicted this way.

Anyhow, a CP prediction constructed directly from such observables will be mostly model independent and therefore ideal for template-based CP detection efforts. It will have small angular scale structures that should also permit the usage of interferometer data that usually lack large angular scale sensitivity. While using this CP template map, it should just be kept in mind that it resembles an educated guess for the galactic CP morphology, and is certainly not accurate in all details. It should, however, be a very helpful template for the extraction of a detectable signal out of the probably noisy CP data and help to verify the detection of the Galactic CP signal by discriminating this from instrumental systematics that plague the measurement of weak polarization signals.

C. Testing the charge of the emitters

The rotational sense of the CP flux should typically have the opposite sign of that of the Faraday rotation if both are measured with the same convention and if the relativistic and thermal particles involved have the same charge sign, e.g. are both electrons. The reason is that the CP sense should directly reflect the gyro-motion of the relativistic particles emitting the radio emission. Faraday rotation is caused by the different phase speeds of left and right polarised electromagnetic waves in a magnetized plasma. The waves that co-rotate with the lightest thermal charge carriers – usually the electrons – can interact most strongly with them and gets the largest delay. Consequently, a linear wave that can be regarded as a superposition of left and right circular waves gets rotated in the sense of the faster wave, and therefore counter rotates with respect to the gyro-motion of the light charge carriers. Thus, if the involved thermal and relativistic particles have the same charge sign, CP and Faraday rotation produced in the same magnetic field counter rotate. This opens the possibility to test for the existence of regions with positrons dominating the radio synchrotron emission.

D. Structure of the paper

The structure of the paper is the following. Sect. II presents the theoretical derivation of the CP pre-

diction map construction. Sect. III provides the predicted CP sky and discusses its remaining model uncertainties. Sect. IV investigates the detectability of the predicted signal and Sect. V concludes.

II. CIRCULAR POLARIZATION SKY

A. Observables

The CP intensity as characterized by Stokes V for a given LOS is approximately given by

$$V = \alpha_V \int dl n_{\text{rel}} B_{\parallel} B_{\perp}^{3/2}, \quad (1)$$

where

$$\alpha_V = -\frac{0.342 \cdot e^{9/2}}{\pi \sqrt{2\pi} \nu^{3/2} m_e c^{7/2} (\gamma_{\text{min}}^{-2} - \gamma_{\text{max}}^{-2})} \quad (2)$$

is a constant, which depends only on natural constants, model parameters and the CP-observational frequency ν [3]. The symbols e , m_e and c denote the elementary charge, the electron mass, and the speed of light, respectively. The relativistic electrons with density n_{rel} are assumed here to have the same power law-like spectrum with cut offs γ_{min} and γ_{max} and spectral index of $p_e = -3$ everywhere. B_{\parallel} is the LOS-parallel, and B_{\perp} the LOS-perpendicular magnetic field component and we wrote $\int dl = \int_{\text{LOS}} dl$ for the LOS integration. Also by writing $B_{\perp}^{3/2}$ we assumed implicitly an electron power law index of $p_e = -3$, which is not too far from the one observed. However, this simplification could be dropped if needed by replacing $B_{\perp}^{3/2}$ with $B_{\perp}^{-p_e/2}$ everywhere, for the price of more contrived calculations. As we only strive for a rough estimate of the CP signal, we will continue with the simpler $B_{\perp}^{3/2}$ scaling.

The building blocks of the CP signal n_{rel} , B_{\parallel} , and B_{\perp} appear in nearly the same combination in the Galactic total synchrotron intensity I and the Faraday depth ϕ ,

$$I = \alpha_I \int dl n_{\text{rel}} B_{\perp}^2, \quad (3)$$

$$\phi = \alpha_{\phi} \int dl n_{\text{th}} B_{\parallel}. \quad (4)$$

Here,

$$\alpha_I = \frac{e^4}{6\pi m_e^2 c^3 \nu (\gamma_{\text{min}}^{-2} - \gamma_{\text{max}}^{-2})} \quad (5)$$

[3] and

$$\alpha_{\phi} = \frac{e^3}{2\pi m_e^2 c^4} \quad (6)$$

[32] are other constants, which depend on similar natural constants and model parameters as α_V , and n_{th}

is the density of free thermal electrons. In particular, the data combination

$$d = \phi I = \alpha_\phi \alpha_I \int dl \int dl' n_{\text{th}}(l) n_{\text{rel}}(l') B_{\parallel}(l) B_{\perp}^2(l') \quad (7)$$

contains the same magnetic field components as $V = \alpha_V \int dl n_{\text{rel}}(l) B_{\parallel}(l) B_{\perp}^{3/2}(l)$, although with slightly different spatial dependence and a slightly different B_{\perp} dependence. If the magnetic field would be spatially constant along a LOS, d and V would be correlated according to

$$\frac{V}{d} = \frac{\alpha_V}{\alpha_\phi \alpha_I} \frac{1}{\int dl n_{\text{th}} B_{\perp}^{1/2}}, \quad (8)$$

so that knowing d would allow us to predict V apart from the weak B_{\perp} dependence, assuming we know the LOS integrated thermal electron density from other measurements like pulsar dispersions. In reality, d and V will not be perfectly correlated as there are unknown magnetic structures on the LOS. The ratio

$$\frac{V}{d} = \frac{\alpha_V}{\alpha_\phi \alpha_I} \frac{\int dl n_{\text{rel}} B_{\parallel} B_{\perp}^{3/2}}{(\int dl n_{\text{th}} B_{\parallel}) (\int dl n_{\text{rel}} B_{\perp}^2)} \quad (9)$$

therefore encodes information on magnetic structures along the LOS, in particular on the co-spatiality of Faraday rotating and synchrotron emitting regions. This information would be interesting to obtain in order to improve our GMF models.

Before CP observations can be exploited for studying Galactic magnetism, the CP signal has to be detected. For this, a rough model of the CP sky would be extremely helpful, as it can be used to build optimal detection templates to be applied to the noisy CP data. In the following, we construct such a predictive CP-polarization all sky map for this purpose. As d is already an observable today, it can be used to predict V to some degree.

V and d will in general be correlated. The production of CP is inevitably associated with total intensity emission and the sign of the produced V is determined by the sign of B_{\parallel} , which always also imprints into the Faraday depth (for emission locations with thermal electrons). This correlation might be weak, in case the synchrotron emission and Faraday depth signals are mostly created at distinct locations with mostly uncorrelated magnetic LOS component B_{\parallel} . If, on the other hand, synchrotron emissions and Faraday rotation are mainly co-spatial, a strong correlation between V and d can be expected. The fact that the Galactic radio emission exhibits strong signatures of Faraday depolarization [1] supports the idea of an intermixed Faraday rotating and synchrotron emitting medium, which promises a large cross-correlation of d and V . Thus the prospects for predicting the CP sky signal to some degree are good.

B. Model

All three observables under consideration here, I , ϕ , and V , could be predicted for a given Galactic model

in $n = (n_{\text{th}}, n_{\text{rel}})$ and $\vec{B} = (B_{\parallel}, \vec{B}_{\perp})$, where we have chosen the LOS direction to be always our first coordinate. Although we have rough models for the 3D Galactic electron distributions n , the full 3D GMF configuration is currently poorly known. The existing GMF models [17–26] largely exploit the available Faraday and synchrotron data and therefore do not contain too much in addition to what these data-sets have to offer. The additional information of these models is due to the usage of parametric models of the GMF spiral structure, which are inspired from the observations of other galaxies. Although this is certainly helpful information, the price to be paid for it is a loss of small-scale structure in the model prediction as the parametric models do not capture all complexity of the data sets they are fitted to. These small-scale structures are, however, extremely important for detecting the Galactic CP signal, as many radio telescopes and in particular radio interferometers are insensitive to large-scale angular structures. Furthermore, a GMF model based prediction is only superior on large scales if the included additional assumptions were correct. Although, this might well be the case, to have a more model independent prediction is certainly healthy.

For these reasons, we will try to predict the CP sky from existing I and ϕ sky maps directly, using only a minimal set of absolutely necessary model assumptions, which we describe now. The inclusion of more information and assumptions is in principle possible and would lead to more sophisticated V -map predictions as we are aiming for here.

As the fluctuations in our observables are mainly caused by magnetic field structures and to a lesser degree by structures in the electron densities $n = (n_{\text{th}}, n_{\text{rel}})$, for which rough, but sufficiently accurate models exist, we will assume n to be known along any given LOS. For n_{th} we adopt the large-scale structure of the popular NE2001 model [27] and n_{rel} is modeled as a thick exponential disc, with parameters as specified in detail in Sec. III. Adapting a simplistic model for the electron densities means that any structure in the RM sky, which is a consequence of not modeled structures in the thermal electron density, will be attributed to magnetic field structures and imprints on the resulting CP sky. Thus, the predicted CP sky will show some features not being present in the real CP sky. Not modeled structures in the relativistic electron density will imprint to both, the total intensity map and the CP map. Therefore, those will imprint on the CP prediction despite the fact that the inference model assigns them to magnetic sub-structures internally.

Although the detailed GMF is still a matter of research, reasonable guesses for how the magnetic energy density scales typically with Galactic locations as expressed through n exist and will be adopted here. This means, we assume that the GMF energy density is largely a function of the electron density. We therefore need an expression for

$$\overline{B}^2(n) = \langle \vec{B}^2 \rangle_{(\vec{B}|n)} \quad (10)$$

with $\langle f(x, y) \rangle_{(x|y)} = \int dx \mathcal{P}(x|y) f(x, y)$ expressing the

probabilistic expectation value of a function $f(x, y)$ (here \bar{B}^2) averaged over the conditional probability $\mathcal{P}(x|y)$ of an unknown variable x (here \vec{B}) given a known variable y (here n to characterize the different typical environments in the Galaxy).

In this work, a simple parametrization of the form

$$\bar{B}^2(n) = \frac{B_0^2}{n_{\text{th}0}^{\beta_{\text{th}}} n_{\text{rel}0}^{\beta_{\text{rel}}}} n_{\text{th}}^{\beta_{\text{th}}} n_{\text{rel}}^{\beta_{\text{rel}}} = B_0^2 x_{\text{th}}^{\beta_{\text{th}}} x_{\text{rel}}^{\beta_{\text{rel}}} \quad (11)$$

will be used, with $x_i \equiv n_i/n_{i0}$ and plausible scaling indices of $\beta = (\beta_{\text{th}}, \beta_{\text{rel}}) \in [0, 1]^2$. To be definitive, we adopt $\beta_{\text{th}} = 0$ and $\beta_{\text{rel}} = 1$ to model our intuition that the observed thick synchrotron disk of the Milky Way and other galaxies probably require magnetic fields which have a thick disk as well as the relativistic electrons causing this thick disk emission. This is in line with the expectation that the relativistic fluid in galaxies, consisting of mainly of relativistic protons, other ions, and electrons, drags magnetic fields with it when it streams out of galactic disks.

In order to show to which degree our CP sky prediction depends on this assumption we also show results for the complementary case $\beta = (1, 0)$. It will turn out that β has only a marginal effect on our prediction, indicating also that the 3D modeling of the electron distributions is not the most essential input to our calculation. The exact normalization of the scaling relation Eq. 11 is given by the parameters $B_0^2, n_{\text{th}0}^{\beta_{\text{th}}}$ and $n_{\text{rel}0}^{\beta_{\text{rel}}}$. In the explicit calculation later on we use $B_0 \approx 6 \mu\text{G}$ and $n_{\text{th}0} \approx 5 \cdot 10^{-2} \text{cm}^{-3}$. The parameter for the relativistic electron density $n_{\text{rel}0}$ drops out later on in the course of the calculation and is therefore left unspecified. The reason for this is that it affects the observable I in exactly the same way as the predicted quantity V , and therefore becomes irrelevant when conditioning our prediction on the observable I , which contains the necessary information on $n_{\text{rel}0}$.

We will exploit the correlation of V with the quantity $d = \phi I$ to predict the former. These quantities depend on the magnetic field structure along a LOS in different ways. Their cross-correlation depends on the magnetic field correlation tensor

$$M_{ij}(\vec{x}, \vec{y}) = \langle B_i(\vec{x}) B_j(\vec{y}) \rangle_{(\vec{B})} \quad (12)$$

as well as on higher correlations functions. A priori, we have no reason to assume that within a roughly homogeneous Galactic environment (as defined by roughly constant n) any direction or location to be singled out. Thus, a statistical homogeneous, isotropic, and mirror-symmetric correlation tensor should model our a priori knowledge about the field, which then is of the form [37]

$$\begin{aligned} M_{ij}(\vec{x}, \vec{y}) &= M_{ij}(\vec{r}) \\ &= M_{\text{N}}(r) \delta_{ij} + (M_{\text{L}}(r) - M_{\text{N}}(r)) \hat{r}_i \hat{r}_j, \end{aligned} \quad (13)$$

with $M_{\text{N}}(r)$ and $M_{\text{L}}(r)$ normal and longitudinal scalar correlation functions, which depend only on the magnitude r of the distance vector $\vec{r} = \vec{x} - \vec{y}$ with normalized components $\hat{r}_i = r_i/r$. These functions describe

the correlation of the field at one location with that at another location shifted in a normal or longitudinal direction with respect to the local magnetic field orientation. These correlation functions are connected due to $\vec{\nabla} \cdot \vec{B} = 0$ via

$$M_{\text{N}}(r) = \frac{1}{2r} \frac{d}{dr} [r^2 M_{\text{L}}(r)] \quad (14)$$

and can be combined into the magnetic scalar correlation $w(r) = \langle \vec{B}(\vec{x}) \cdot \vec{B}(\vec{x} + \vec{r}) \rangle_{(\vec{B})} = 2M_{\text{N}}(r) + M_{\text{L}}(r)$ so that $\bar{B}^2 = w(0) = 2M_{\text{N}}(0) + M_{\text{L}}(0)$ [37].

In our calculations, only correlations along of LOSs are needed, leading to the restriction $\vec{r} = (r, 0, 0)$ if we identify the LOS direction with the first coordinate axis. This implies a component-wise diagonal correlation structure

$$\begin{aligned} M_{ij}(\vec{r})|_{\vec{r}=(r,0,0)} &= [M_{\text{N}}(r) + (M_{\text{L}}(r) - M_{\text{N}}(r)) \delta_{i1}] \delta_{ij} \\ &= \begin{pmatrix} M_{\text{L}} & 0 & 0 \\ 0 & M_{\text{N}} & 0 \\ 0 & 0 & M_{\text{N}} \end{pmatrix}_{ij}(r) \end{aligned} \quad (15)$$

and therefore no a priori expectation of any cross-correlation of B_{\parallel} and B_{\perp} along a given LOS. This simplifies the calculation of higher order magnetic correlation functions. For such we will use the Wick theorem, e.g.

$$\langle B_i B_j B_k B_l \rangle_{(\vec{B})} = M_{ij} M_{kl} + M_{ik} M_{jl} + M_{il} M_{jk},$$

and therefore implicitly a Gaussian probability for the magnetic field components. The real magnetic field statistics is most likely non-Gaussian, leading to differences between our estimated higher order correlates and the real ones. However, since we do not know how to model this non-Gaussianity correctly as we do not know even the sign of its effect on higher order correlations, and as we also like to keep the complexity of our calculations moderate we accept this simplification. We expect only a moderate and global multiplicative change of order unity on our predicted CP sky if the nature of non-Gaussianity would be known and taken into account in the prediction, as non-Gaussianity corrections would roughly affect all LOSs more or less similarly.

Furthermore, we assume the longitudinal and normal magnetic correlation lengths (defined here differently to match our later needs)

$$\begin{aligned} \lambda_{\text{L}} &= \int dr M_{\text{L}}(r)/M_{\text{L}}(0) \text{ and} \\ \lambda_{\text{N}} &= \int dr M_{\text{N}}^2(r)/M_{\text{N}}^2(0) \end{aligned} \quad (16)$$

to be much smaller than typical variations in the underlying electron density profiles, so that e.g. the expected Faraday dispersion can be calculated via

$$\begin{aligned} \langle \phi^2 \rangle_{(\vec{B}|n)} &= \alpha_{\phi}^2 \int_0^{\infty} dl \int_0^{\infty} dl' n_{\text{th}}(l) n_{\text{th}}(l') \langle B_{\parallel}(l) B_{\parallel}(l') \rangle_{(\vec{B}|n)} \\ &\approx \alpha_{\phi}^2 \int_0^{\infty} dl \int_{-\infty}^{\infty} dr n_{\text{th}}(l) n_{\text{th}}(l+r) M_{\text{L}}(r) \\ &\approx \frac{1}{3} \alpha_{\phi}^2 \lambda_{\text{L}} \int_0^{\infty} dl n_{\text{th}}^2 \bar{B}^2(n). \end{aligned} \quad (17)$$

We introduced the notation $f(l) = f(l\hat{r}_{\text{LOS}})$ for the value of the 3D field $f(\vec{r})$ along the LOS coordinate l in direction \hat{r}_{LOS} . Here, and in the following we will treat the individual LOSs separately. Furthermore, we assumed that magnetic structures are smaller than the part of the LOS that resides in the Galaxy as expressed in terms of the structure of the adopted thermal electron model, so that a negligible error is implied by extending the integration over the relative distances $r = l' - l$ from minus to plus infinity or by using the same thermal electron density for both locations, l and $l + r$. Furthermore, we used $M_{\text{L}}(0) = M_{\text{N}}(0) = \frac{1}{3}\bar{B}^2$, which follows from isotropy and Eq. 15.

Finally, we assume the observed Faraday and total intensity skies to be noiseless. This approximation will simplify the CP sky estimator and make it independent of the normalization of the scaling relation Eq. 11 and the actual value of the correlation length λ_{L} as long this does not vary (strongly) along a given LOS. The assumed correlations length λ_{N} will have some small impact on our result, however, of sub-dominant order and therefore it is also not necessary to specify it if only a rough CP sky prediction is required.

C. Estimator

We want to exploit the correlation of V with $d = \phi I$ to construct an optimal linear estimator for V given d . This is given by

$$\bar{V} = \langle V d \rangle_{(\bar{B}|n)} \langle d^2 \rangle_{(\bar{B}|n)}^{-1} d \quad (18)$$

irrespective of the underlying statistics, since one can easily show that the quadratic error expectation $\epsilon^2 = \langle [V - \bar{V}(d)]^2 \rangle_{(\bar{B}|n)}$ is always minimized for linear estimators of the form $\bar{V}(d) = v d$ for $v = \langle V d \rangle_{(\bar{B}|n)} \langle d^2 \rangle_{(\bar{B}|n)}^{-1}$:

$$\begin{aligned} \frac{d\epsilon^2}{dv} &= -2 \langle [V - v d] d \rangle_{(\bar{B}|n)} \\ &= 2 \left[v \langle d^2 \rangle_{(\bar{B}|n)} - \langle V d \rangle_{(\bar{B}|n)} \right] = 0. \end{aligned} \quad (19)$$

All remaining analytical work is to calculate the correlates which compose v . The simpler one is

$$\begin{aligned} \langle d^2 \rangle_{(\bar{B}|n)} &= \langle \phi^2 I^2 \rangle_{(\bar{B}|n)} \\ &= \alpha_\phi^2 \alpha_I^2 \int dl_1 \dots \int dl_4 n_{\text{th}1} n_{\text{th}2} n_{\text{rel}3} n_{\text{rel}4} \times \\ &\quad \langle B_{||1} B_{||2} B_{\perp 3}^2 B_{\perp 4}^2 \rangle_{(B|n)} \\ &= \alpha_\phi^2 \alpha_I^2 \int dl_1 \dots \int dl_4 n_{\text{th}1} n_{\text{th}2} n_{\text{rel}3} n_{\text{rel}4} \times \\ &\quad M_{\text{L}12} [M_{\text{N}33} M_{\text{N}44} + 2 M_{\text{N}34}^2] \\ &\approx \frac{1}{27} \lambda_{\text{L}} \alpha_\phi^2 \alpha_I^2 \left[\int dl n_{\text{th}}^2 \bar{B}^2 \right] \times \\ &\quad \left[\left(\int dl n_{\text{rel}} \bar{B}^2 \right)^2 + 2 \lambda_{\text{N}} \int dl n_{\text{rel}}^2 \bar{B}^4 \right] \end{aligned} \quad (20)$$

Here, we used the abbreviations $n_{\text{th}1} = n_{\text{th}}(l_1)$, $B_{||2} = B_{||}(l_2)$, $M_{\text{N}34} = M_{\text{N}}(l_3 - l_4)$, and the like, exploited

the diagonal structure of the magnetic correlations along the LOS as expressed by Eq. 15 while applying the Wick theorem, and inserted the correlation lengths λ_{L} and λ_{N} as defined in Eq. 16 while applying the short correlation length approximation as previously used in Eq. 17.

The calculation of $\langle V d \rangle_{(\bar{B}|n)}$ is slightly more complicated. To handle the $B_{\perp}^{3/2}$ dependence of V , we Taylor expand it in terms of B_{\perp}^2 around $B_{\perp 0}^2 = \frac{2}{3} B_0^2$ via

$$\begin{aligned} B_{\perp}^{3/2} &= (B_{\perp}^2)^{3/4} = \sum_{n=0}^{\infty} \binom{3/4}{n} B_{\perp 0}^{2(\frac{3}{4}-n)} (B_{\perp}^2 - B_{\perp 0}^2)^n \\ &= \binom{3/4}{0} B_{\perp 0}^{3/2} + \binom{3/4}{1} B_{\perp 0}^{-\frac{1}{2}} (B_{\perp}^2 - B_{\perp 0}^2) + \mathcal{O}(B_{\perp}^4) \\ &\approx \frac{1}{4} B_{\perp 0}^{3/2} + \frac{3}{4} B_{\perp 0}^{-1/2} B_{\perp}^2. \end{aligned} \quad (21)$$

We choose to expand in B_{\perp}^2 rather than B_{\perp} , as the linear terms would vanish anyway during the application of the Wick theorem.

We then find:

$$\begin{aligned} \langle V d \rangle_{(\bar{B}|n)} &= \langle V \phi I \rangle_{(\bar{B}|n)} \\ &= \alpha_V \alpha_\phi \alpha_I \int dl_1 \dots \int dl_3 n_{\text{th}1} n_{\text{rel}2} n_{\text{rel}3} \times \\ &\quad \langle B_{||1} B_{||2} B_{\perp 2}^{\frac{3}{2}} B_{\perp 3}^2 \rangle_{(B|n)} \\ &\approx \alpha_V \alpha_\phi \alpha_I \int dl_1 \dots \int dl_3 n_{\text{th}1} n_{\text{rel}2} n_{\text{rel}3} \times \\ &\quad \left\langle B_{||1} B_{||2} \left(\frac{1}{4} B_{\perp 0}^{3/2} + \frac{3}{4} B_{\perp 0}^{-1/2} B_{\perp 2}^2 \right) B_{\perp 3}^2 \right\rangle_{(B|n)} \\ &= \alpha_V \alpha_\phi \alpha_I \int dl_1 \dots \int dl_3 n_{\text{th}1} n_{\text{rel}2} n_{\text{rel}3} \times \\ &\quad \frac{B_{\perp 0}^{-1/2}}{4} M_{\text{L}12} \left(B_{\perp 0}^2 M_{\text{N}33} + \right. \\ &\quad \left. + 3 [M_{\text{N}22} M_{\text{N}33} + 2 M_{\text{N}23}^2] \right) \\ &\approx \frac{B_{\perp 0}^{-\frac{1}{2}}}{36} \lambda_{\text{L}} \alpha_V \alpha_\phi \alpha_I \times \\ &\quad \left[B_{\perp 0}^2 \left(\int dl n_{\text{th}} n_{\text{rel}} \bar{B}^2 \right) \left(\int dl n_{\text{rel}} \bar{B}^2 \right) \right. \\ &\quad \left. + \left(\int dl n_{\text{th}} n_{\text{rel}} \bar{B}^4 \right) \left(\int dl n_{\text{rel}} \bar{B}^2 \right) + \right. \\ &\quad \left. 2 \lambda_{\text{N}} \int dl n_{\text{th}} n_{\text{rel}}^2 \bar{B}^6 \right]. \end{aligned} \quad (22)$$

Again we used $M_{\text{L}}(0) = M_{\text{N}}(0) = \frac{1}{3}\bar{B}^2$ and λ_{L} and λ_{N} as defined in Eq. 16. This gives us in Gaussian units

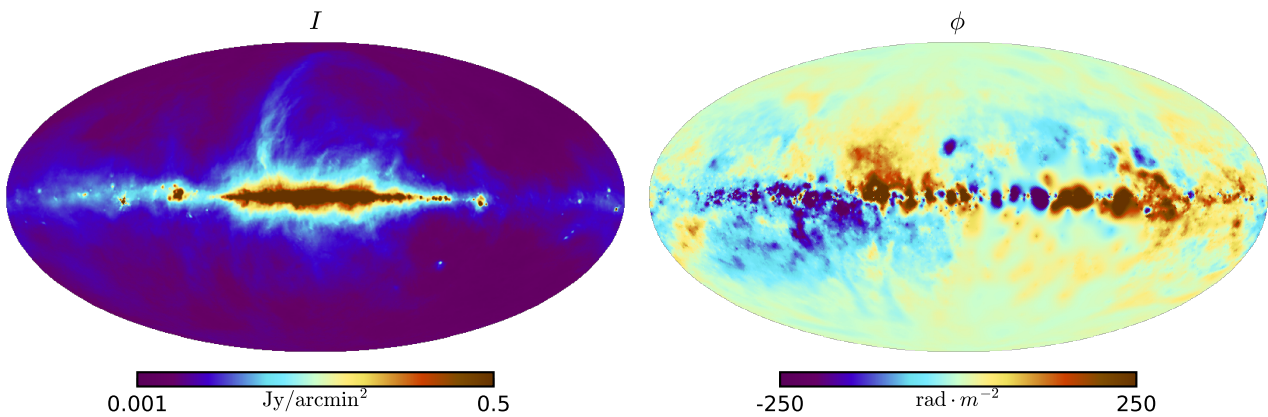


Figure 1. Left: Synchrotron intensity at 408 MHz as provided by [38]. Right: Faraday rotation map as constructed by [32]. Red indicates magnetic fields predominantly pointing towards the observer and clockwise rotation of the received linear polarisation. This is according to the IAU convention for measuring angles and is therefore opposite to the mathematical convention.

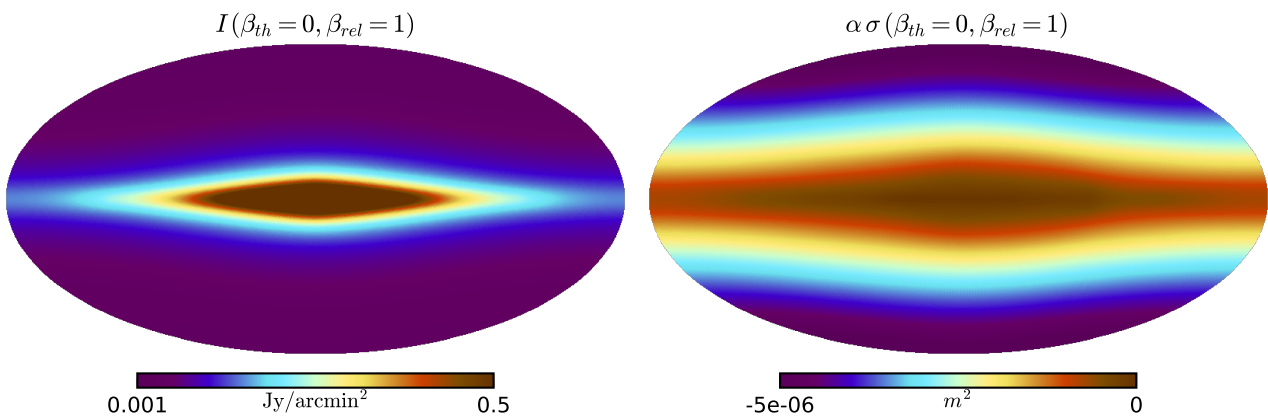


Figure 2. Left: Synchrotron emission intensity at 408 MHz of the simplistic 3D model. Right: Map of the resulting conversion factor $\alpha\sigma$, which translates the Faraday rotation map ϕ into the fractional CP map V/I at 408 MHz. For both the relativistic electron profile of Eq. 27 and $\beta = (0, 1)$ were assumed.

being a LOS-independent dimensionless quantity and

$$\sigma = \left(\int dl n_{\text{th}}^2 \bar{B}^2 \right)^{-1} \times \left[\left(\int dl n_{\text{rel}} \bar{B}^2 \right)^2 + 2\lambda_{\text{N}} \int dl n_{\text{rel}}^2 \bar{B}^4 \right]^{-1} \times \left[\frac{2}{3} B_0^2 \left(\int dl n_{\text{rel}} \bar{B}^2 \right) \left(\int dl n_{\text{th}} n_{\text{rel}} \bar{B}^2 \right) + \left(\int dl n_{\text{rel}} \bar{B}^2 \right) \left(\int dl n_{\text{th}} n_{\text{rel}} \bar{B}^4 \right) + 2\lambda_{\text{N}} \int dl n_{\text{th}} n_{\text{rel}}^2 \bar{B}^6 \right] \quad (25)$$

$$\bar{V} = \alpha \sigma \phi I, \quad \text{with} \quad (23)$$

$$\alpha = \frac{3\alpha_{\text{V}}}{4\alpha_{\phi}\alpha_{\text{I}}B_{\perp 0}^{1/2}} \approx -4.269 \cdot \sqrt{\frac{m_{\text{e}}^3 c^7}{e^5 \nu B_0}} \approx -2.189 \cdot 10^{18} \left(\frac{\nu}{408 \text{ MHz}} \right)^{-1/2} \left(\frac{B_0}{6 \mu\text{G}} \right)^{-1/2} \quad (24)$$

a LOS-dependent constant with dimension of an area. The unknown λ_{L} canceled out and the unknown λ_{N} affects only sub-dominant terms, as it is e.g. compared in the denominator to the Galactic dimension $L = \left(\int dl n_{\text{rel}} \bar{B}^2 \right)^2 / \left(\int dl n_{\text{rel}}^2 \bar{B}^4 \right) \gg \lambda_{\text{N}}$. We therefore neglect terms proportional to λ_{N} in the following

and calculate

$$\begin{aligned} \sigma &\approx \frac{\frac{2}{3} B_0^2 \int dl n_{\text{th}} n_{\text{rel}} \bar{B}^2 + \int dl n_{\text{th}} n_{\text{rel}} \bar{B}^4}{\left(\int dl n_{\text{th}}^2 \bar{B}^2 \right) \left(\int dl n_{\text{rel}} \bar{B}^2 \right)} \\ &\approx \frac{\frac{2}{3} \int dl x_{\text{th}}^{1+\beta_{\text{th}}} x_{\text{rel}}^{1+\beta_{\text{rel}}} + \int dl x_{\text{th}}^{1+2\beta_{\text{th}}} x_{\text{rel}}^{1+2\beta_{\text{rel}}}}{n_{\text{th}0} \left(\int dl x_{\text{th}}^{2+\beta_{\text{th}}} x_{\text{rel}}^{\beta_{\text{rel}}} \right) \left(\int dl x_{\text{th}}^{\beta_{\text{th}}} x_{\text{rel}}^{1+\beta_{\text{rel}}} \right)} \end{aligned} \quad (26)$$

for each LOS to translate $d = \phi I$ into \bar{V} there.

III. PREDICTION

To give an estimate for the CP sky, we need maps of the total synchrotron intensity and the Faraday rotation of the Milky Way. We use the 408 MHz map provided by [38], which is based on the data of [39–42], and the Faraday rotation map provided by [32], which is largely based on the data of [43]. These are shown in Fig. 1

We further need to quantify the σ parameter given in Eq. 26. For this we need the thermal and relativistic electron distribution of the galaxy and thereby x_{rel} and x_{th} . For the 3D distribution of the thermal electron density in the Milky Way we use the NE2001 model [27] without its local features. The spatial and the energy distribution of relativistic electrons in the Galaxy are more uncertain as we have only direct measurements of the cosmic ray electrons near the Earth. Considerable effort to infer these distributions have been made [29–35]. As we have shown in Eq. 26, we only need the spatial dependence and not the actual normalisation of n_{rel} , which means that this quantity only effects the relative strength of different structures in the CP map and not the overall strength of the predicted CP intensity itself. For this reason, and since we only aim for a rough estimate, we are content with a simplistic large-scale relativistic electron model. Given the distribution of matter in the galaxy, an exponential model for the spatial structure of cosmic ray electrons may make sense, as already adopted by other authors ([2, 17, 21, 44]), at least in a similar way. In our case, we can use Eqs. 3 and 11 to give an estimate of the of total synchrotron map given our relativistic electron model and the scaling parameters of Eq. 11, where we adopt $\beta = (0, 1)$ and try to reproduce the large scale pattern of the 408 MHz map shown in Fig. 1. We thereby choose the following model for the spatial dependence of the relativistic electrons:

$$x_{\text{rel}} = e^{-|\vec{r}|/r_0} \cdot \cosh^{-2}(|\vec{z}|/z_0) \quad (27)$$

The vector \vec{r} points in the radial direction in the galactic plane, the vector \vec{z} points out of the plane. As mentioned before, the parameters r_0 and z_0 are estimated via a naive comparison of the observed and estimated synchrotron maps at 408 MHz shown in Figs. 1 and 2, respectively. The parameters adapted in this work are $r_0 = 12$ kpc and $z_0 = 1.5$ kpc. Given the morphological complexity of the map in relation

to the simplicity of the model and the poorly understood nature of the origin and evolution of electron cosmic rays we acknowledge that the parameters of this model are highly uncertain. Also completely different parametrization of x_{rel} might lead to the same estimate for I because of the projection involved. The conversion factor $\alpha \sigma$ implied by our rough 3D model at 408 MHz is also shown in 2 for $\beta = (0, 1)$.

The resulting estimate of the circular polarisation intensity of the Milky Way is depicted in Figs. 3 for the two cases $\beta = (0, 1)$ and $\beta = (1, 0)$. The morphology of the resulting maps is dominated by the morphology of the Faraday and the synchrotron map, what seems natural given our formalism. The influence of the dependence of the magnetic field on the different electron densities seems to be small, as the difference between between the two complementary cases is negligible, as we show for the predicted V/I ratio in Fig. 4. We predict a signal of up to $5 \cdot 10^{-4}$ Jansky per square arcminute at 408 MHz and more at lower frequencies. The CP is strongest in the center plane of the Galaxy. The relative strength of the CP intensity to the total synchrotron intensity up to $V/I \sim 3 \cdot 10^{-4}$ as depicted in Fig. 4. The V/I ratio is largest just above and below the disc, as well as in some spots in the outer disc. We expect this ratio to increase with $\nu^{-0.5}$, approaching 10^{-3} at 40 MHz, which might be a detectable level for current instrumentation[45]. The frequency scaling of $V/I \propto \nu^{-0.5}$ was already predicted by [36] for the GHz range.

The diffusion length of relativistic electrons depends on energy, therefore, the radio sky at different frequencies is not just a rescaled version of the 408 MHz map used as a template here. The V/I map provided by this work, however, should – within its own limitations – be valid at others frequencies as well. Therefore, it can be used after scaling by $(\nu/408 \text{ MHz})^{-0.5}$ to translate total intensity templates at other frequencies into CP expectation maps at the same frequency, which then incorporate any difference of the radio sky due to spatially varying relativistic electron spectra.

Anyhow, even if a total intensity template is not available at the measurement frequency, the main structure of the CP prediction, which are the sign changes induced by the sign changes of the Faraday sky, will be robust with respect to a change in frequency. Therefore, the CP template should be used as a structure expected on the sky, while allowing the real sky to deviate by some factor from it due to errors induced by the assumed frequency scaling and other simplifications. A template search method that is robust in this respect, is discussed below.

The assumed scaling of the magnetic field energy density with the electron densities, β has only a minor impact on the result. The difference between the $\beta = (0, 1)$ and the $\beta = (1, 0)$ scenarios is less than 10%, as Fig. 4 shows. Together with Fig. 5 this is indeed evidence for the robustness of our results, as the profiles of relativistic and thermal electrons used in this work are quite different, nonetheless the different scaling does not lead to significantly different CP maps.

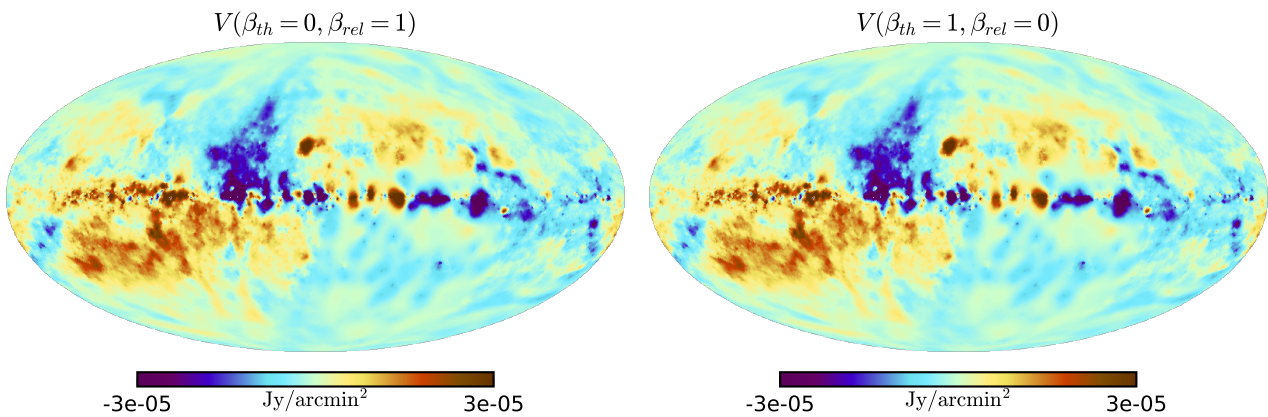


Figure 3. Predicted circular polarisation intensity at 408 MHz for $\beta = (0, 1)$ (left) and $\beta = (1, 0)$. Red indicates clockwise rotation, according to the IAU convention for measuring angles that is opposite to the mathematical convention.

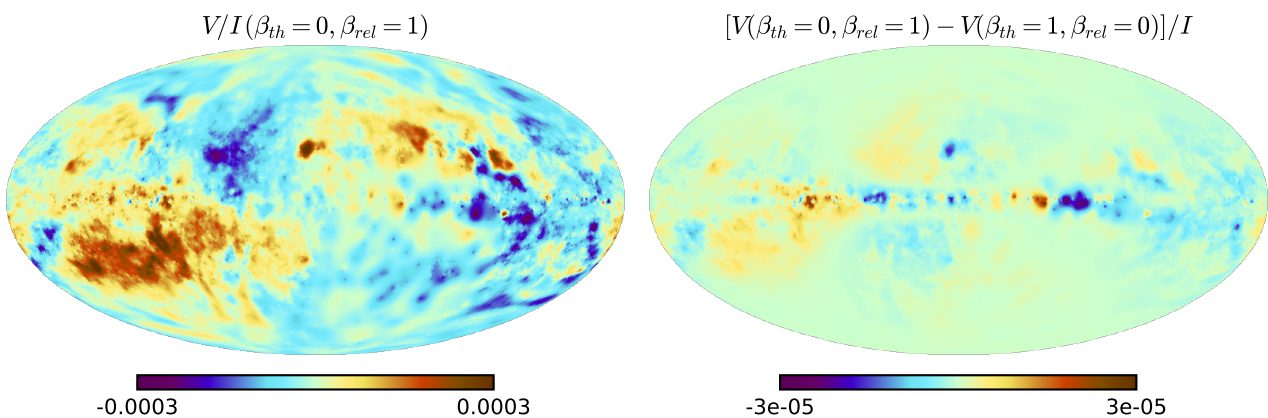


Figure 4. Predicted V/I ratio at 408 MHz for $\beta = (0, 1)$ (left) and the difference of the $\beta = (0, 1)$ and $\beta = (1, 0)$ ratios (right).

IV. DETECTION STRATEGY

A. Traditional imaging

Now, we investigate the possibility to detect this CP signal with single-dish and interferometric observations, by requiring a signal-to-noise ratio of 10 in CP and by assuming a Stokes- V to I sensitivity ratio of $\sigma_V/\sigma_I \approx \sqrt{2}$ and a power-law total intensity frequency spectrum ($I_\nu \propto \nu^\alpha$, with $\alpha = -0.8$). For example, the Sardinia Radio Telescope has the capability to observe in the low portion of the electromagnetic spectrum: in P-band (305 – 410 MHz) and in L-band (1.3 – 1.8 GHz). By using the specifications given in [46], an observing time of $\lesssim 1$ s per beam is required to reach the requested sensitivity in both frequency bands.

One of the largest surveys of the sky at the moment available is the NRAO VLA Sky Survey (NVSS, [47]) characterized by a sensitivity in Stokes U and Q of 0.29 mJy/beam. The sensitivity at this frequency and resolution to detect the signal we are interested in is $\approx 6 \mu\text{Jy}/\text{beam}$. In principle, such a sensitivity can be reached by stacking all the 2326 fields of the survey if

one can assume $\sigma_V \approx \sigma_Q \approx \sigma_U$.

We performed a similar evaluation for the LOFAR and the SKA, by referring to the lowest frequency band available for these instruments. For LOFAR, we use 45 MHz, where we expect $V/I \approx 0.001$. At this frequency, the required sensitivity is reached in less than 1 s. For the SKA, we considered the SKA-Low specifications given after the re-baselining in the frequency range 50 – 350 MHz, with a central frequency of 200 MHz and a bandwidth of 300 MHz. The required sensitivity can be reached in 3 h of observing time, if a resolution of ≈ 7 arcsec is considered. The Effelsberg telescope should obtain enough sensitivity within 20 minutes observation in its 400 MHz band and the GMRT within 30 min in its 200 MHz band.

Thus, the prospects to detect the predicted CP signal are good from a pure signal to noise perspective. However, the polarization accuracy after calibration of the new generation of radio telescopes is typically of 0.1 – 1 % [e.g. 48, 49]. This instrumental limitation will make the imaging of the CP signal extremely hard as contamination of the CP signal by polarization leakage will be in the best case as strong as the signal we predict, in many cases one or two orders of

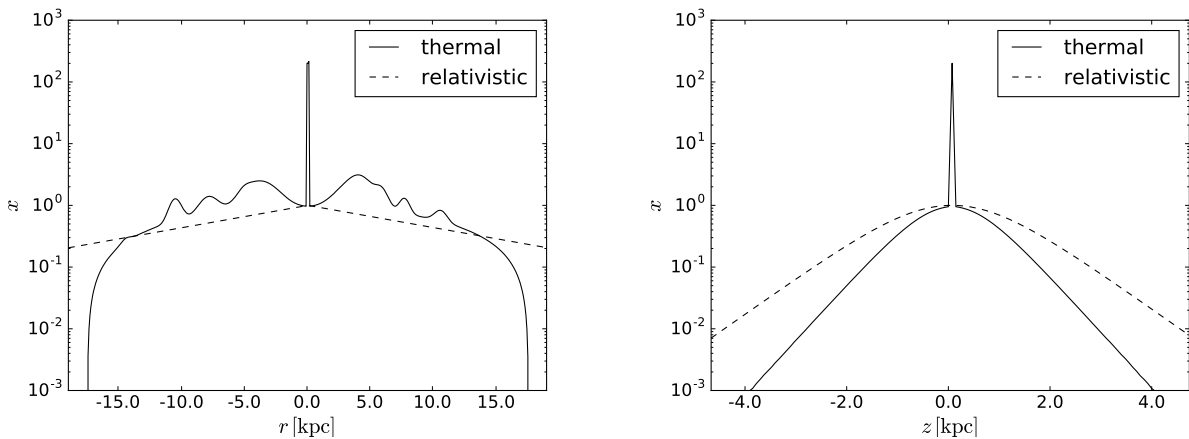


Figure 5. Profiles of the thermal and relativistic electron density used in this work in terms of the dimensionless quantities x_{th} and x_{rel} as defined in the context of Eq. 11.

magnitude stronger.

To overcome this, we propose to cross-correlate the measured CP sky with our predicted one, as such instrumental effects are not present in our prediction and therefore should statistically averaged out in the comparison.

B. Template search

The CP all sky prediction constructed in the previous section can be used to search for the weak Galactic CP signal even in strongly contaminated data. Although CP sky images are usually not available, a number of radio telescopes take circular polarization data

$$d_V = \int_{S^2} d\hat{n} R(\hat{n}) V(\hat{n}) + \xi. \quad (28)$$

Here, $d_V = (d_{V1}, \dots, d_{Vu}) \in \mathbb{C}^u$ is the data vector of length u . \hat{n} is a direction on the celestial sphere S^2 . $R : S^2 \rightarrow \mathbb{C}^u$ is the CP instrument response encoding the primary beam, the Fourier transform of the sky and subsequent sampling in case of interferometers, and any gain factors of the telescope. $V(\hat{n})$ is the CP sky and $\xi \in \mathbb{C}^u$ is the noise vector of the observation including the cross talk from other Stokes parameters. Here, we assume ξ to be generated by a zero-mean stochastic process with known covariance $\Xi = \langle \xi \xi^\dagger \rangle_{(\xi)}$, which has to be obtained by careful studying the instrumental properties.

Some part of the observed data vector can now be predicted using the CP prediction $\bar{V}(\hat{n})$, namely

$$\bar{d}_V = R \bar{V} = \alpha \int_{S^2} d\hat{n} R(\hat{n}) \sigma(\hat{n}) \phi(\hat{n}) I(\hat{n}). \quad (29)$$

Since our prediction might be off by some multiplicative factor due to the various approximations involved in its derivation, and since we did not attempt to calculate the model uncertainty, a comparison via a likelihood function $\mathcal{P}(d_V | \bar{d}_V)$ is out of reach. However, a simple, but sensitive indicator function (or test statistics) for the presence of the predicted CP signal

is the inversely noise-weighted scalar-product of observed and predicted data,

$$t = \bar{d}_V^\dagger \Xi^{-1} d_V. \quad (30)$$

If $V = \gamma \bar{V} + \delta V$ is the correct CP sky, with $\gamma \sim 1$ the factor necessary to correct for our approximations, δV the CP structures missed by our prediction due to imperfect correlation of V with $d = \phi I$, and $U = \langle \delta V \delta V^\dagger \rangle_{(\bar{B}, n)}$ the imperfection covariance, we expect

$$\begin{aligned} \bar{t} &= \langle t \rangle_{(\bar{B}, \xi | n)} = \gamma \bar{V}^\dagger R^\dagger \Xi^{-1} R \bar{V} > 0 \text{ and} \\ \sigma_t^2 &= \langle (t - \bar{t})^2 \rangle_{(\bar{B}, \xi | n)} = u + \text{Tr} [U R^\dagger \Xi^{-1} R] \end{aligned} \quad (31)$$

and therefore a signal-to-noise ratio (SNR) of

$$\frac{S}{N} = \frac{\bar{t}^2}{\sigma_t^2} = \frac{\gamma^2 \left(\text{Tr} [R \bar{V} \bar{V}^\dagger R^\dagger \Xi^{-1}] \right)^2}{u + \text{Tr} [R U R^\dagger \Xi^{-1}]}, \quad (32)$$

where we used $\text{Tr} [\Xi \Xi^{-1}] = u$, the number of data points. If we only reconstructed $f = 10\%$ of the intensity of the true celestial CP signal, so that $\gamma^2 \langle \bar{V} \bar{V}^\dagger \rangle \approx f^2 U = 10^{-2} U$, and if the CP data is 99% ($= 1 - p$) noise and cross leakage dominated, so that $R \langle V V^\dagger \rangle R^\dagger \approx R U R^\dagger \approx p^2 \Xi \approx 10^{-4} \Xi$, we get a SNR of $S/N \approx f^2 p^2 u = 10^{-12} u$ and enter the detection range ($S/N \sim 1$) in the terabyte regime ($u \sim f^{-2} p^{-2} = 10^{12}$).

V. CONCLUSIONS

Using the observational information on magnetic fields along and perpendicular to the LOS from Faraday rotation and synchrotron total emission we provided a detailed map of the expected diffuse Galactic CP emission², which is at a level of $3 \cdot 10^{-3}$ of the total

² The V and V/I maps for the two scenarios discussed are available at <http://wwwmpa.mpa-garching.mpg.de/ift/data/CP01/>.

intensity at 408 MHz and higher at lower frequencies. This prediction relies on assumptions about the magnetic field statistics, and the three dimensional distributions of thermal and relativistic electrons throughout the Milky Way. As these assumptions are not certain, the real Galactic CP sky can and will differ from our prediction. Nevertheless, the provided CP prediction can be used for template based searches for the elusive CP signal. Our model shows similarities and differences to a CP prediction based on a 3D models of the Milky Way [36]. We expect our model to capture more details of the real CP sky, as its construction is based directly on observed data sets, without the detour of using those to construct a parametrized, and therefore coarse, 3D model. However, which model is more accurate should certainly be answered by observations.

A confirmation of the celestial CP signal we predict would indicate a co-location of the origin of the observed Faraday rotation signal and synchrotron emission. In case the predicted signal is not detectable with a strength comparable to the prediction, this would indicate a spatial separation of these regions along the LOSs and therefore important information on the Galactic magnetic field structure and its correlation with thermal and relativistic electrons.

Finally, we like to point out that the hypothetical possibility exist that the observed CP signal has the opposing sign compared to our prediction (even after potential confusions of the used CP conventions are eliminated). This would happen in case the synchrotron emission of the Milky Way would predominantly result from relativistic positrons, which gyrate in the opposite direction compared to the electrons. This is – however – very unlikely given that the observed local density of relativistic electrons is much higher than that of the positrons and given that the relativistic particles in the Milky Way are believed to be accelerated out of the thermal particle pool. Nevertheless, it shows that the charge of the Galactic synchrotron emitters can actually be tested by sensitive CP observations.

ACKNOWLEDGMENTS

This research was supported by the DFG Forschungsgruppe 1254 “Magnetisation of Interstellar and Inter-galactic Media: The Prospects of Low-Frequency Radio Observations”. We thank Henrik Junklewitz and Rick Perley for discussions and an anonymous referee for constructive feedback.

-
- [1] M. Wolleben, T. L. Landecker, W. Reich, and R. Wielebinski, *A&A* **448**, 411 (2006), astro-ph/0510456.
 - [2] L. Page, G. Hinshaw, E. Komatsu, M. R.olta, D. N. Spergel, C. L. Bennett, C. Barnes, R. Bean, O. Doré, J. Dunkley, et al., *ApJS* **170**, 335 (2007), astro-ph/0603450.
 - [3] A. Pandya, Z. Zhang, M. Chandra, and C. F. Gammie, *ApJ* **822**, 34 (2016), 1602.08749.
 - [4] G. C. Bower, H. Falcke, and D. C. Backer, *ApJ* **523**, L29 (1999), astro-ph/9907215.
 - [5] R. J. Sault and J.-P. Macquart, *ApJ* **526**, L85 (1999), astro-ph/9910052.
 - [6] R. Fender, D. Rayner, R. Norris, R. J. Sault, and G. Pooley, *ApJ* **530**, L29 (2000), astro-ph/9911425.
 - [7] R. P. Fender, D. Rayner, D. G. McCormick, T. W. B. Muxlow, G. G. Pooley, R. J. Sault, and R. E. Spencer, *MNRAS* **336**, 39 (2002), astro-ph/0204442.
 - [8] T. W. Jones and S. L. Odell, *ApJ* **214**, 522 (1977).
 - [9] T. W. Jones and S. L. Odell, *ApJ* **215**, 236 (1977).
 - [10] P. E. Hodge, *ApJ* **263**, 595 (1982).
 - [11] E. Valtaoja, *Ap&SS* **100**, 227 (1984).
 - [12] M. M. Komesaroff, J. A. Roberts, D. K. Milne, P. T. Rayner, and D. J. Cooke, *MNRAS* **208**, 409 (1984).
 - [13] C.-I. Björnsson, *MNRAS* **242**, 158 (1990).
 - [14] T. Beckert and H. Falcke, *A&A* **388**, 1106 (2002), astro-ph/0112398.
 - [15] M. Ruszkowski and M. C. Begelman, *ApJ* **573**, 485 (2002), astro-ph/0112090.
 - [16] T. A. Enßlin, *A&A* **401**, 499 (2003), astro-ph/0212387.
 - [17] X. H. Sun, W. Reich, A. Waelkens, and T. A. Enßlin, *A&A* **477**, 573 (2008), 0711.1572.
 - [18] A. Waelkens, T. Jaffe, M. Reinecke, F. S. Kitaura, and T. A. Enßlin, *A&A* **495**, 697 (2009), 0807.2262.
 - [19] R. Jansson, G. R. Farrar, A. H. Waelkens, and T. A. Enßlin, *JCAP* **7**, 021 (2009), 0905.2228.
 - [20] T. R. Jaffe, J. P. Leahy, A. J. Banday, S. M. Leach, S. R. Lowe, and A. Wilkinson, *MNRAS* **401**, 1013 (2010), 0907.3994.
 - [21] X.-H. Sun and W. Reich, *Research in Astronomy and Astrophysics* **10**, 1287 (2010), 1010.4394.
 - [22] L. Fauvet, J. F. Macías-Pérez, J. Aumont, F. X. Désert, T. R. Jaffe, A. J. Banday, M. Tristram, A. H. Waelkens, and D. Santos, *A&A* **526**, A145 (2011), 1003.4450.
 - [23] T. R. Jaffe, A. J. Banday, J. P. Leahy, S. Leach, and A. W. Strong, *MNRAS* **416**, 1152 (2011), 1105.5885.
 - [24] R. Jansson and G. R. Farrar, *ApJ* **757**, 14 (2012), 1204.3662.
 - [25] R. Jansson and G. R. Farrar, *ApJ* **761**, L11 (2012), 1210.7820.
 - [26] Planck Collaboration, *A&A* **596**, A103 (2016), 1601.00546.
 - [27] J. M. Cordes and T. J. W. Lazio, *ArXiv Astrophysics e-prints* (2002), astro-ph/0207156.
 - [28] M. Greiner, D. H. F. M. Schnitzeler, and T. A. Enßlin, *A&A* **590**, A59 (2016), 1512.03480.
 - [29] A. W. Strong and I. V. Moskalenko, *Advances in Space Research* **27**, 717 (2001), astro-ph/0101068.
 - [30] A. W. Strong, I. V. Moskalenko, and O. Reimer, *ApJ* **613**, 962 (2004), astro-ph/0406254.
 - [31] A. E. Vladimirov, S. W. Digel, G. Jóhannesson, P. F. Michelson, I. V. Moskalenko, P. L. Nolan, E. Orlando, T. A. Porter, and A. W. Strong, *Computer Physics Communications* **182**, 1156 (2011), 1008.3642.
 - [32] N. Oppermann, H. Junklewitz, G. Robbers, M. R. Bell, T. A. Enßlin, A. Bonafede, R. Braun, J. C. Brown, T. E. Clarke, I. J. Feain, et al., *A&A* **542**, A93 (2012), 1111.6186.
 - [33] E. Orlando, A. W. Strong, I. V. Moskalenko, C. Dickinson, S. Digel, T. R. Jaffe, G. Jóhannesson, J. P.

- Leahy, T. A. Porter, and M. Vidal, ArXiv e-prints (2015), 1507.05958.
- [34] M. N. Mazziotta, F. Cerutti, A. Ferrari, D. Gaggero, F. Loparco, and P. R. Sala, *Astroparticle Physics* **81**, 21 (2016), 1510.04623.
- [35] C. Evoli, D. Gaggero, A. Vittino, G. Di Bernardo, M. Di Mauro, A. Ligorini, P. Ullio, and D. Grasso, *JCAP* **2**, 015 (2017), 1607.07886.
- [36] S. King and P. Lubin, *Phys. Rev. D* **94**, 023501 (2016), 1606.04112.
- [37] K. Subramanian, *Physical Review Letters* **83**, 2957 (1999), astro-ph/9908280.
- [38] M. Remazeilles, C. Dickinson, A. J. Banday, M.-A. Bigot-Sazy, and T. Ghosh, *MNRAS* **451**, 4311 (2015), 1411.3628.
- [39] C. G. T. Haslam, M. J. S. Quigley, and C. J. Salter, *MNRAS* **147**, 405 (1970).
- [40] C. G. T. Haslam, W. E. Wilson, D. A. Graham, and G. C. Hunt, *A&AS* **13**, 359 (1974).
- [41] C. G. T. Haslam, U. Klein, C. J. Salter, H. Stoffel, W. E. Wilson, M. N. Cleary, D. J. Cooke, and P. Thomasson, *A&A* **100**, 209 (1981).
- [42] C. G. T. Haslam, C. J. Salter, H. Stoffel, and W. E. Wilson, *A&AS* **47**, 1 (1982).
- [43] A. R. Taylor, J. M. Stil, and C. Sunstrum, *ApJ* **702**, 1230 (2009).
- [44] R. Drimmel and D. N. Spergel, *The Astrophysical Journal* **556**, 181 (2001), astro-ph/0101259.
- [45] I. Myserlis, E. Angelakis, A. Kraus, C. A. Liontas, N. Marchili, M. F. Aller, H. D. Aller, V. Karamanavis, L. Fuhrmann, T. P. Krichbaum, et al., ArXiv e-prints (2017), 1706.04200.
- [46] I. Prandoni, M. Murgia, A. Tarchi, M. Burgay, P. Castangia, E. Egron, F. Govoni, A. Pellizzoni, R. Ricci, S. Righini, et al., ArXiv e-prints (2017), 1703.09673.
- [47] J. J. Condon, W. D. Cotton, E. W. Greisen, Q. F. Yin, R. A. Perley, G. B. Taylor, and J. J. Broderick, *AJ* **115**, 1693 (1998).
- [48] R. A. Perley and B. J. Butler, *ApJS* **206**, 16 (2013), 1302.6662.
- [49] M. Murgia, F. Govoni, E. Carretti, A. Melis, R. Concu, A. Trois, F. Loi, V. Vacca, A. Tarchi, P. Castangia, et al., *MNRAS* **461**, 3516 (2016), 1607.03636.